Coordinate roles for collagen VI and biglycan in regulating tendon collagen fibril structure and function

Ryan J. Leiphart [b,1], **Hai Pham** [a,1], **Tyler Harvey** [d], **Taishi Komori** [a], **Tina M. Kilts** [a], **Snehal S. Shetye** [b], **Stephanie N. Weiss** [b], **Sheila M. Adams** [c], **David E. Birk** [c], **Louis J. Soslowsky** [b] and **Marian F. Young** [a,*]

a - *National Institute of Dental and Craniofacial Research,* National Institutes of Health, Bethesda, MD 20892, USA
b - *McKay Orthopedic Research Laboratory,* University of Pennsylvania, Philadelphia, PA, USA
c - *University of South Florida,* Morsani College of Medicine, Tampa, FL 33612, USA
d - *Carnegie Institution for Science,* Department of Embryology, The Johns Hopkins University, USA

Correspondence to Marian F. Young: myoung@nidcr.nih.gov *(M.F. Young)*
https://doi.org/10.1016/j.mbplus.2021.100099

Abstract

Tendon is a vital musculoskeletal tissue that is prone to degeneration. Proper tendon maintenance requires complex interactions between extracellular matrix components that remain poorly understood. Collagen VI and biglycan are two matrix molecules that localize pericellularly within tendon and are critical regulators of tissue properties. While evidence suggests that collagen VI and biglycan interact within the tendon matrix, the relationship between the two molecules and its impact on tendon function remains unknown. We sought to elucidate potential coordinate roles of collagen VI and biglycan within tendon by defining tendon properties in knockout models of collagen VI, biglycan, or both molecules. We first demonstrated co-expression and co-localization of collagen VI and biglycan within the healing tendon, providing further evidence of cooperation between the two molecules during nascent tendon matrix formation. Deficiency in collagen VI and/or biglycan led to significant reductions in collagen fibril size and tendon mechanical properties. However, collagen VI-null tendons displayed larger reductions in fibril size and mechanics than seen in biglycan-null tendons. Interestingly, knockout of both molecules resulted in similar properties to collagen VI knockout alone. These results indicate distinct and non-additive roles for collagen VI and biglycan within tendon. This work provides better understanding of regulatory interactions between two critical tendon matrix molecules.

Introduction

Tendon is a unique tissue that connects muscle to bone and is therefore critical in transmitting forces for skeletal movement and stability. Tendon pathology, with origins ranging from genetic mutations to physical overuse and injury, presents a significant clinical problem for a wide range of patients[1–3]. Due to the poor self-healing capacity of tendons, tissue engineering and other therapeutic approaches to tendon repair have been largely unsuccessful. Better understanding of the functional interplay between tendon matrix and cell biology is needed to augment current tendon pathology treatment paradigms.

While the tendon extracellular matrix (ECM) is dominated by collagen I fibrils, the matrix is composed of a diverse set of other collagens and proteins. Collagen I fibrils play a dominant role in dictating tendon mechanical strength; however, these fibrils are tightly regulated by other collagens and non-collagenous proteins present in

tendon [4–6]. Previous studies have shown that matrix molecules interact to properly organize collagen I fibrils and maintain tendon mechanical integrity [7–10]. The fundamental mechanisms by which these ECM components cooperatively maintain tendon function, however, are unknown.

Small leucine-rich proteoglycans (SLRPs), such as biglycan, are critical matrix regulators in many skeletal and non-skeletal tissues [11,12]. SLRPs consist of a small core protein containing leucine rich repeats (LRR) and attached glycosaminoglycan (GAG) chains. Previous studies demonstrate that the LRR motifs in the SLRP core protein permit binding to fibrillar and non-fibrillar collagens, thereby regulating collagen fibril growth and assembly [13]. In tendon, these SLRPs, especially biglycan, are key regulators of mechanical and structural properties. Biglycan deficiency results in irregular collagen fibril architecture [8,14]. Such changes correspond with decreased tendon mechanical properties and joint function [15–19]. Previous work also implicates biglycan in regulating tendon stem cell fate [20]. While biglycan has been shown to be a key regulator of tendon physiology, the ECM interactions behind this functional regulation remain elusive.

Collagen VI is another abundant matrix component in tendons. This non-fibrillar collagen molecule is composed of three interwoven α-chains with a central triple helical domain and terminal non-collagenous domains. These molecules assemble into tetramers before forming an extracellular "beaded microfilament" network [21]. Prior research shows that collagen VI interacts with numerous ECM components, including collagen I, collagen II, decorin, and biglycan [22–24]. Collagen VI often localizes to pericellular regions of musculoskeletal tissues suggesting it has roles related to cell-matrix interactions [25–28]. In this context it is theorized that collagen VI may serve as a "bridge" between cells and the ECM, thereby playing important roles in cell mechanosensation and cell surface growth factor modulation. Mutations in genes encoding collagen VI cause Bethlem myopathy or Ullrich congenital muscular dystrophy (UCMD), which manifest with muscular weakness and connective tissue abnormalities [29]. In cartilage, collagen VI is the main component of the pericellular matrix (PCM) which is a key structure for mechanotransduction and for maintaining proper cell function [26]. Collagen VI has been shown to influence proper collagen fibril assembly and regulate tendon function [25]. However, the specific role(s) of collagen VI in tendon remain understudied.

In addition to their individual roles in regulating tendon function, evidence suggests that biglycan and collagen VI may interact with each other within the matrix. When combined *in vitro*, biglycan binds to collagen VI and organizes the fibrils into a hexagonal, mesh-like network [30]. This filamentous network resembles a pericellular matrix previously observed in tendon [31]. This dual-molecule structure suggests that biglycan and collagen VI function cooperatively within tendon. Therefore, the objective of this study was to define the impact of biglycan and collagen VI on tendon structural and functional properties using single or combined knockout models. We hypothesized that the two molecules have epistatic roles, and that a dual knockout would lead to further decreases in tendon properties than depletion of either molecule alone.

Results

Expression of collagen VI and biglycan in healing tendons

To clarify how collagen VI and biglycan might cooperate within tendon, we assessed their co-expression and co-localization within healing tendons, as tendon healing recapitulates aspects of tendon matrix formation[32–34]. Upregulation in gene expression and protein presence during healing therefore suggests similar patterns and potential function through other tendon matrix contexts, including formation or growth. We used a mouse tendon injury punch model [35] and performed bulk RNA-Seq in weekly intervals throughout the subsequent healing process. Temporal RNA-Seq revealed that increases in *Bgn* transcripts corresponded with increases in transcripts encoding the three primary collagen VI genes (*Col6a1*, *Col6a2*, and *Col6a3*) (Fig. 1A). RNA expression of these genes rose above uninjured control levels by 1-week post-injury, peaked at 2-weeks post-injury, and returned to uninjured levels by 4-weeks post-injury. Unsupervised clustering of *Bgn* and *Col6* RNA-Seq data grouped 1- and 2-weeks post-injury samples together, further supporting upregulation of these genes during these healing time-points (Supplemental Fig. 1). These expression dynamics are consistent with many injury-responsive tendon genes [36]. *De novo* tendon matrix formation occurs within the first two weeks following injury. Elevated *Bgn* and *Col6a1, Col6a2, and Col6a3* expression during this healing window suggests that biglycan and the dominant a_1(VI) a_2(VI)a_3(VI) form of collagen VI play key roles in tendon matrix formation during repair. We next sought to visualize where collagen VI and biglycan proteins localize within healing tendons. Immunohistochemistry on serial sections of the healing patellar tendon showed enrichment for both molecules in and around the injury site, further implying critical roles of these molecules in regulating nascent tendon matrix production (Fig. 1B).

Collagen fibril structure

We elucidated the structural impact of loss of biglycan, collagen VI, or both molecules on
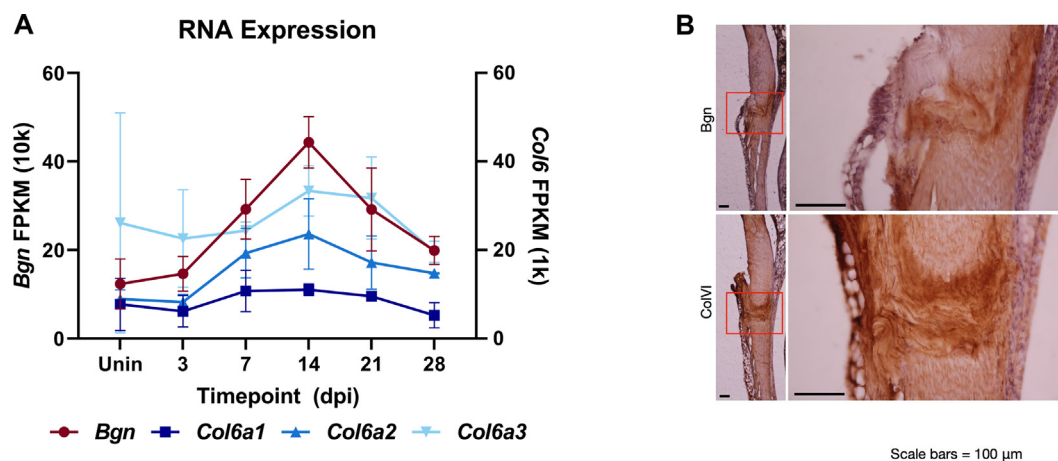
Fig. 1. Collagen VI and biglycan co-expression and co-localization in healing tendon. A. Relative fragments per kilobase million (FPKM) RNA counts for *Bgn* (left axis) and *Col6* (right axis) genes reveals consistent injury-responsive expression patterns in these genes. Following injury, expression of these genes rises above uninjured levels by 1-week post-injury, peaks at 2-weeks post-injury, and returns to near-baseline levels by 4-weeks post-injury. Results are from isolated tendon pairs (n = 3 tendons). B. Immunohistochemistry staining of ColVI and Bgn on post-injury tendon sections at low magnification (left image) and high magnification of red inset (right image). Healing biopsy punch site is boxed in red in lower magnification image. Size bars = 100 μm. (For interpretation of the references to color in this figure legend, the reader is referred to the web version of this article.)

collagen fibril architecture in mature tendons. The models used were global knockouts of biglycan ($Bgn^{-/0}$) and/or collagen VI ($Col6a2^{-/-}$), the latter of which results in a total loss of collagen VI trimer secretion [37,38]. TEM images of FDL tendon sections were analyzed from 2 month-old WT, $Bgn^{-/0}$, $Col6a2^{-/-}$, and $Col6a2^{-/-};Bgn^{-/0}$ mice. Our results showed that qualitatively, fibril shape was comparable across groups with roughly circular fibril cross-sections in all 4 genotypes. Fibril diameter distribution in $Bgn^{-/0}$ tendons was similar to that of WT tendons, with a moderate shift towards smaller diameter fibrils (median WT value 138.5 nm vs 111.2 nm in $Bgn^{-/0}$ mice, Fig. 2A&B). Collagen VI deficiency, on the other hand, led to more robust changes in fibril diameter distribution. Both $Col6a2^{-/-}$ and $Col6a2^{-/-};Bgn^{-/0}$ tendons demonstrated marked shifts towards smaller diameter fibrils, with median fibril diameters of 77.7 nm and 72.2 nm, respectively (Fig. 2C&D). While both collagen VI knockout genotypes displayed over representation of the smallest diameter subpopulation (~25–55 nm) compared to WT and $Bgn^{-/0}$ mice, $Col6a2^{-/-};Bgn^{-/0}$ tendons contained a more heterogeneous mix of large and small fibrils than $Col6a2^{-/-}$ tendons. This is evidenced by a larger 3rd quartile fibril diameter in $Col6a2^{-/-};Bgn^{-/0}$ tendons compared to that of $Col6a2^{-/-}$ tendons (126.4 nm vs 109.0 nm, respectively) despite comparable median diameter values. The increased representation of larger fibrils in the double knockout tendons compared to the single collagen VI knockout tendons is interesting, as this would not be predicted by combining the effects of each single knockout model. This result suggests that biglycan and collagen VI play synergistic, rather

than additive, roles in regulating tendon fibril structure. Fibril density (fibril number/μm^2) was significantly increased in single and double KO genotypes compared to WT tendons (Fig. 3B). However, $Col6a2^{-/-}$ tendons had greater fibril density than that of $Bgn^{-/0}$ tendons. This was expected given the larger proportion of smaller fibrils in knockout tendons, especially in the single collagen VI knockout group.

In addition to the fibril changes that resulted from collagen VI and/or biglycan deficiency, we defined the impact of loss of these molecules on tendon cell (tenocyte) morphology within higher order tissue structure. In lower magnification TEM images of healthy WT tendons, tenocytes are organized in uniaxial columns with cellular processes extending perpendicular to the tendon axis and partitioning collagen fibrils within larger fibers (Fig. 4A). In $Bgn^{-/0}$ tendons, this morphology was preserved, as tenocytes exhibited long cytoplasmic processes radiating from the tenocyte body and separating groups of fibrils (Fig. 4B). However, this normal morphology was disrupted in both collagen VI knockout genotypes. Collagen VI-null tenocytes had shortened and disorganized cytoplasmic processes that incompletely partitioned adjacent fibrils (Fig. 4C&D). The surface of these tenocytes was also separated from the pericellular fibrillar matrix, which was not apparent in WT or $Bgn^{-/0}$ tendons. Associated with the poorly developed tenocyte processes, collagen VI-null tendons demonstrated less organized grouping of fibrils into fibers compared to WT and $Bgn^{-/0}$ tendons.
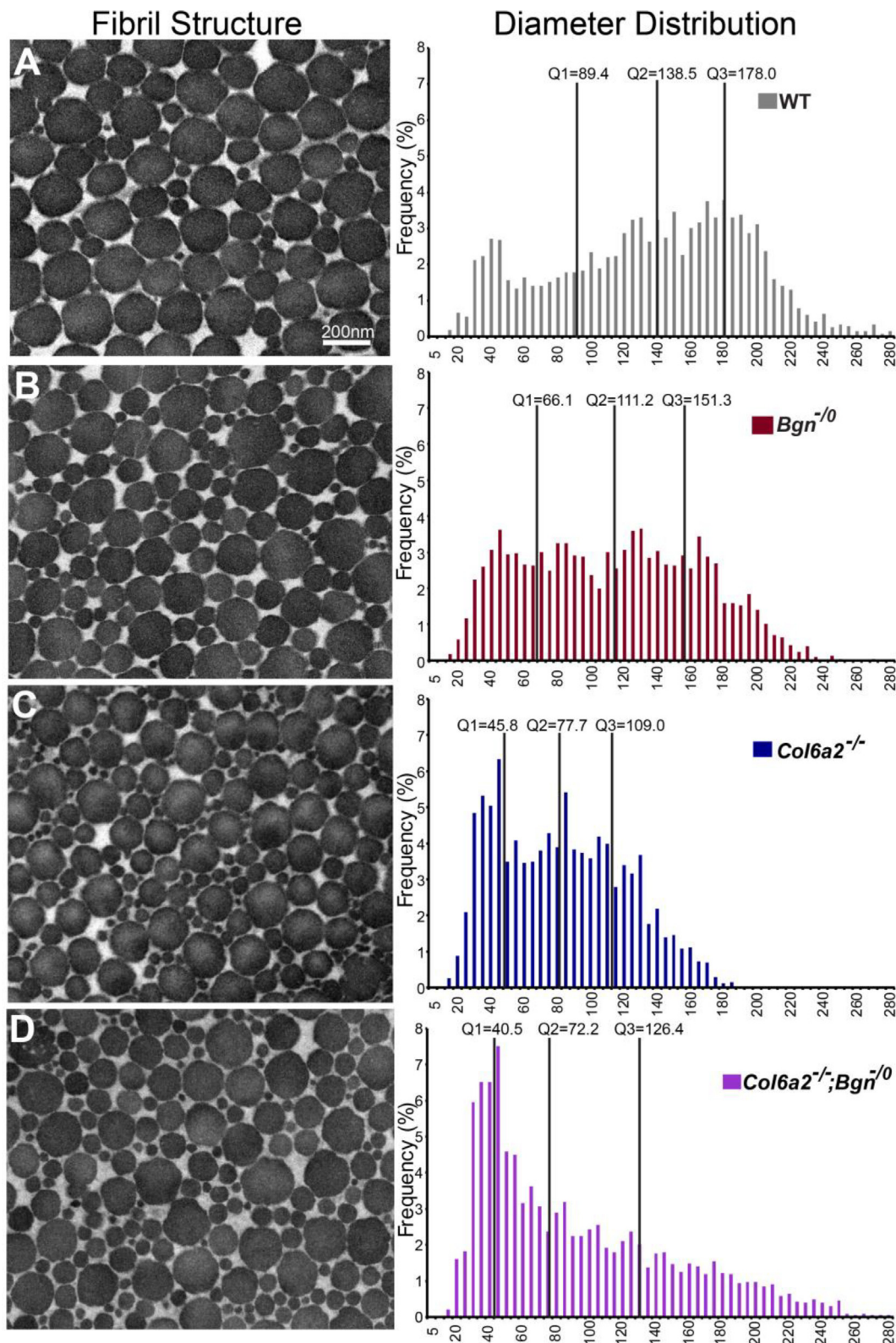
Fig. 2. Collagen fibril diameter in FDL tendons. (A) WT FDL tendons display a bimodal distribution of large (~160 nm diameter) and small (<100 nm diameter) collagen fibrils. (B) *Bgn*[-/0] FDL tendons demonstrated a moderate shift towards smaller fibril diameters while maintaining a bimodal distribution. (C) *Col6a2*^{-/-} FDL tendons contained a significantly larger proportion of small diameter fibrils with decreased presence of large fibrils. (D) While *Col6a2*^{-/-}; *Bgn*[-/0] FDL tendons also displayed a prominent shift towards small diameter fibrils, they contained an increased proportion of larger fibrils compared to *Col6a2*^{-/-} FDL tendons. Fibril measurements were collected across n = 4 tendons/genotype from n ≥ 3 mice/genotype.

Biomechanical characteristics

Given the structural changes to the collagen fibril network seen in collagen VI and biglycan-null tendons, we next tested whether their mechanical properties were affected. Cross-sectional area (CSA) was reduced with loss of biglycan, collagen VI, or both molecules. (Fig. 5A). $Col6a2^{-/-}$ and $Col6a2^{-/-};Bgn^{-/0}$ tendons also had smaller CSA than $Bgn^{-/0}$ tendons. Deficiency in biglycan, collagen VI, or both molecules resulted in weaker tendons without decreasing tendon material properties. Tendons from all knockout genotypes were less stiff and had lower maximum loads than WT tendons (Fig. 5B,C). $Col6a2^{-/-}$ and $Col6a2^{-/-};Bgn^{-/0}$ tendons were less stiff than $Bgn^{-/0}$ tendons, and $Col6a2^{-/-};Bgn^{-/0}$ tendons had lower maximum loads than $Col6a2^{-/-}$ and $Bgn^{-/0}$ tendons. No differences in moduli were observed between any of the groups (Fig. 6A). $Col6a2^{-/-}$ and $Col6a2^{-/-};Bgn^{-/0}$ tendons had higher maximum stresses than WT and $Bgn^{-/0}$ tendons (Fig. 6B). Loss of collagen VI reduced tendon viscoelasticity, as $Col6a2^{-/-}$ and $Col6a2^{-/-};Bgn^{-/0}$ tendons exhibited lower percent relaxation than WT and $Bgn^{-/0}$ tendons (Fig. 6C).

Given the mechanical deficiencies of the knockout tendons, we quantified the collagen fiber realignment dynamics of these tendons in response to load. Biglycan loss led to delayed fiber realignment compared to WT. During the ramp to failure, WT tendons realigned between 3% and 5% strain (Fig. 7A) while $Bgn^{-/0}$ tendons realigned between 5% and 7% strain (Fig. 7B). $Col6a2^{-/-}$ and $Col6a2^{-/-};Bgn^{-/0}$ tendons realigned earlier in response to load, between 1% and 3% strain (Fig. 7C&D). At 3% and 5% strain, $Bgn^{-/0}$ tendons were less aligned than $Col6a2^{-/-}$ and $Col6a2^{-/-};Bgn^{-/0}$ tendons and trended towards less alignment than WT tendons (Supplemental Fig. 2).

This mechanical data demonstrates that both biglycan and collagen VI play critical roles in regulating FDL tendon mechanical properties. Knockout of either molecule, or both in unison, led to reductions in tendon CSA, stiffness, and maximum load. Collagen VI knockout led to larger reductions in mechanical properties than seen in biglycan deficient tissues, suggesting that collagen VI plays a larger role in regulating tendon mechanics. The regulatory roles of collagen VI and biglycan are also distinct. Collagen VI knockout reduced tendon viscoelasticity, while biglycan deficiency did not appreciably impact viscoelasticity. Biglycan loss led to delayed fiber realignment compared to WT tendons, while collagen VI-deficient tendons realigned earlier in the ramp to failure than WT tendons. Despite these distinct roles, the effects of biglycan and collagen VI deficiency on tendon mechanics were not additive. Tendons deficient in both molecules mechanically behaved like tendons deficient in collagen VI alone. While knockout tendons displayed decreased structural-mechanical properties (stiffness and maximum load), these changes did not correspond with changes in modulus. Maximum stress was surprisingly increased in collagen VI knockout tendons, the opposite effect seen with maximum load. These results are in part due to initial differences in tendon geometry. Tendons from all mutant genotypes had reduced size compared to WT tendons, and collagen VI knockout tendons were smaller than both WT and $Bgn^{-/0}$ tendons. In conclusion, both collagen VI and biglycan regulate FDL tendon mechanics, with collagen VI being a more robust effector.

Discussion

Overall, our data indicates that collagen VI and biglycan play critical roles in regulating tendon function that are distinct and non-additive. Injured tendons co-express and co-localize these matrix proteins within the healing tissue. Since tendon healing recapitulates aspects of tendon matrix formation, these results suggest that collagen VI and biglycan may also cooperate during matrix formation of developing tendons. While this experiment analyzed healing tendons rather than developing tendons, our results are corroborated by prior studies demonstrating increased expression of collagen VI and biglycan during early tendon formation [39,40]. Co-expression and co-localization of collagen VI and biglycan during tendon healing also supports prior *in vitro* evidence that the two molecules are capable of binding and interacting in a manner that changes their architecture [24,30].

Despite their co-residence within tendon tissue, loss of collagen VI or biglycan led to different structural and mechanical changes to the tendon. Collagen VI knockout resulted in a larger proportion of small diameter collagen fibrils than seen with biglycan knockout alone. Tenocyte morphology was also perturbed with collagen VI deficiency but was relatively preserved with biglycan knockout alone. These robust structural changes in collagen VI-null tendons corresponded with larger deficits in mechanical properties compared to $Bgn^{-/0}$ tendons. The more robust functional deficits seen in collagen VI-null tendons compared to biglycan-null tendons indicates that the molecules may play different roles in regulating tendon properties, and that collagen VI plays a more substantial regulatory role than that of biglycan. Interestingly, when collagen VI and biglycan were knocked out together, resultant tendon properties closely mimicked those of the collagen VI knockout alone. Aside from increased proportion of larger diameter collagen fibrils and decreased maximum load, no measured properties were statistically different between
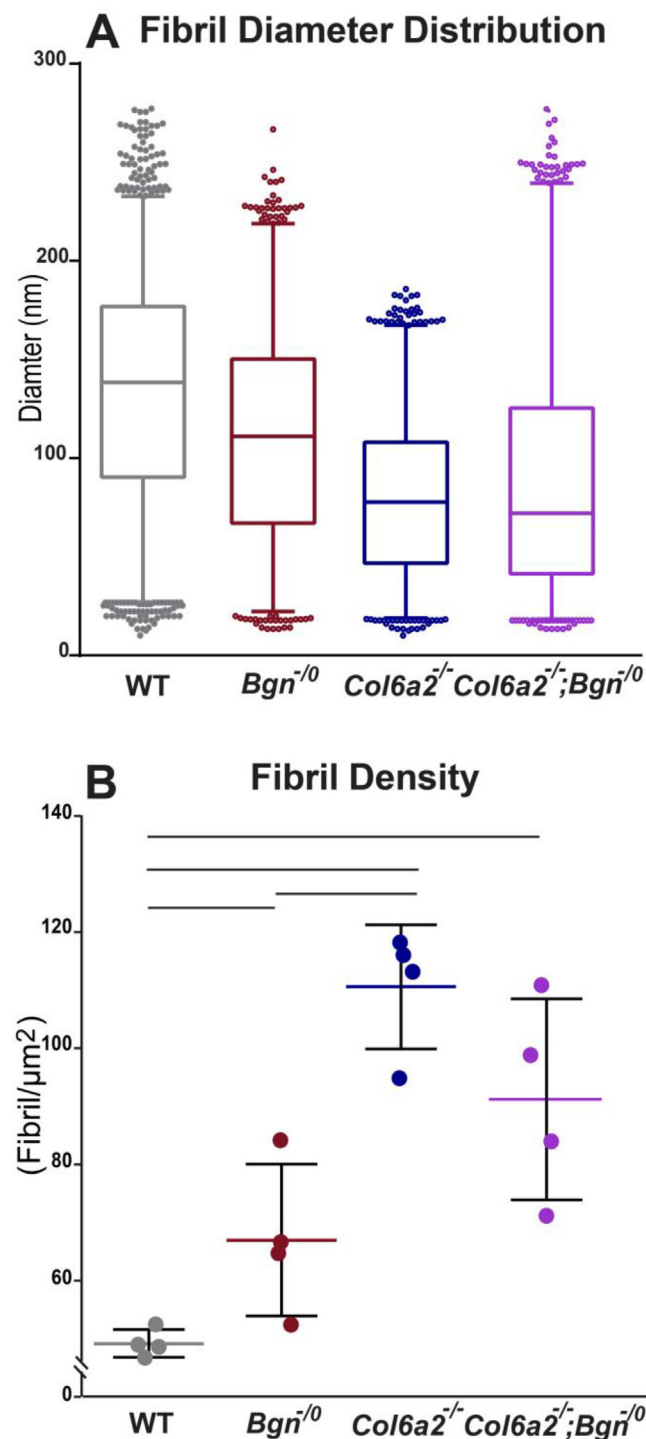
Fig. 3. Collagen fibril size distributions and fibril density. (A) Box and whisker plots of collagen fibril size distributions demonstrate a decrease in the median size of collagen fibrils in FDL knockout tendons. Kolmorogov-Smirnov tests demonstrated that each distribution was distinct from those of all other genotypes (p < 0.001). (B) Given the increased proportion of small diameter fibrils in collagen VI-null tendons, *Col6a2*^{-/-} and *Col6a2*^{-/-}*;Bgn*[-/0] FDL tendons had increased fibril density compared to WT and *Bgn*[-/0] tendons. Bars indicate p < 0.05 for paired Student's t-tests. Fibril measurements were collected across n = 4 tendons/genotype from n ≥ 3 mice/genotype.

Col6a2^{-/-} and *Col6a2*^{-/-}*;Bgn*[-/0] tendons. This demonstrates that the roles of collagen VI and biglycan are not additive, as further loss of biglycan in collagen VI-null tendons did not lead to substantial changes compared to collagen VI single knockout tendons.
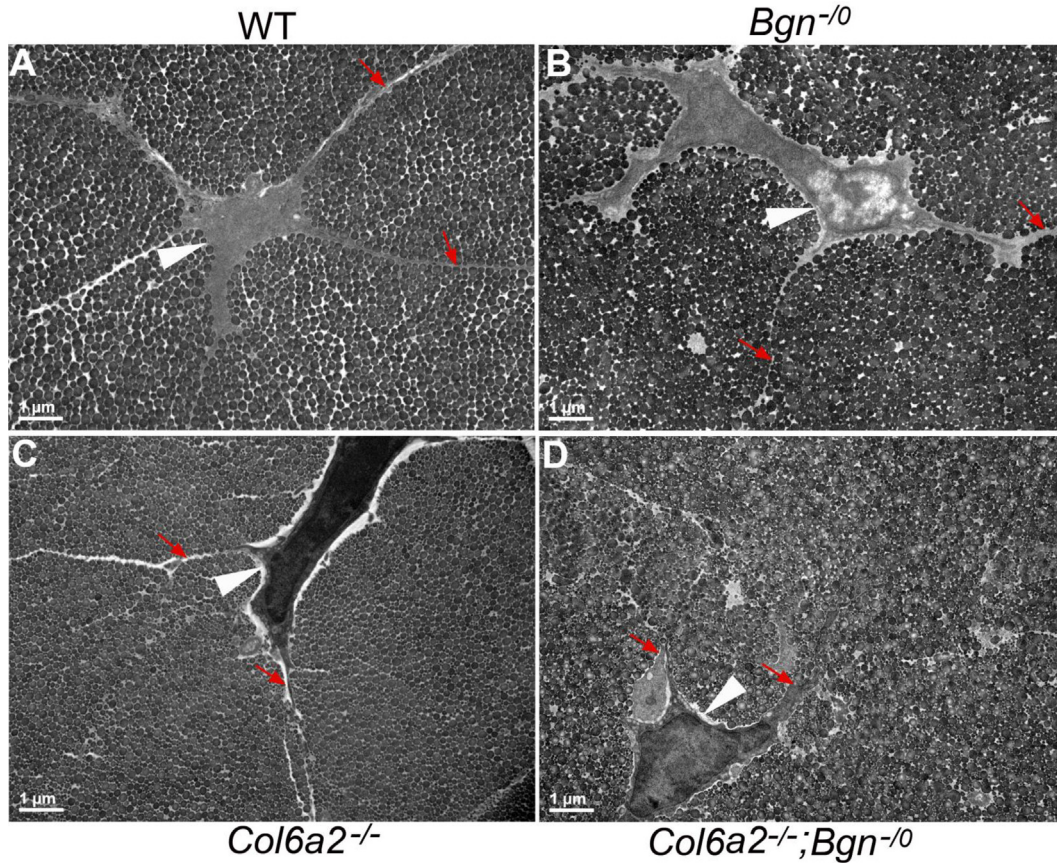
Fig. 4. Tenocyte processes and morphology. Tenocytes are organized into uniaxial columns with processes extending perpendicular to the tendon axis. This higher order tendon structure is comparable in WT and *Bgn$^{-/0}$* tendons with long cytoplasmic processes (red arrows) radiating out from the tenocyte and partitioning the fibrillar matrix. (Fig. 4 A,B). In contrast, both *Col6a2$^{-/-}$* and *Col6a2$^{-/-}$;Bgn$^{-/0}$* tenocytes had shortened, disorganized cytoplasmic processes that incompletely partitioned the adjacent fibers (Fig. 4 C,D). In the collagen VI deficient genotypes, there was a separation of the tenocyte surface from the tendon fibrillar matrix (White arrow heads). This apparent lack of pericellular adhesion was not observed in the WT or *Bgn$^{-/0}$* tendons. In addition, both fibrils and fibers were less organized compared to WT and *Bgn$^{-/0}$* tendons. (For interpretation of the references to color in this figure legend, the reader is referred to the web version of this article.)
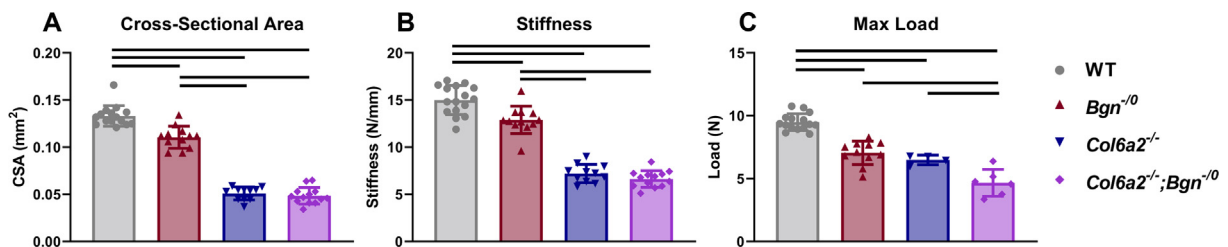

Fig. 5. Cross-sectional area and structural-mechanical properties. (A) WT tendons had a larger CSA than all knockout genotypes. *Bgn$^{-/0}$* tendons had larger CSA than collagen VI knockout tendons. (B) WT tendons were stiffer than all knockout genotypes. *Bgn$^{-/0}$* tendons were stiffer than collagen VI knockout tendons. (C) WT tendons had a higher maximum load than all knockout genotypes. *Bgn$^{-/0}$* and *Col6a2$^{-/-}$* tendons had higher maximum loads than *Col6a2$^{-/-}$;Bgn$^{-/0}$* tendons. Bars indicate $p < 0.05$ from one-way ANOVAs with Bonferroni post-hoc comparisons.

Results of the current study may be explained by proposed models of the tendon pericellular matrix (PCM). When combined *in vitro*, biglycan organizes collagen VI fibrils into a hexagonal mesh-like network, with biglycan occupying vertices within this mesh [30]. This mesh-like net-
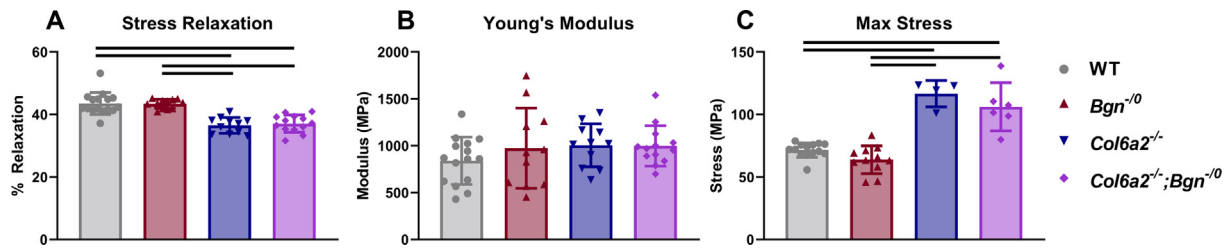
Fig. 6. Material and viscoelastic properties. (A) No differences in moduli were observed between genotypes. (B) Both collagen VI knockout tendons had higher maximum stresses than WT and *Bgn*[-/0] tendons. (C) WT and *Bgn*[-/0] tendons exhibited more stress relaxation than collagen VI knockout tendons. Bars indicate $p < 0.05$ from one-way ANOVAs with Bonferroni post-hoc comparisons.
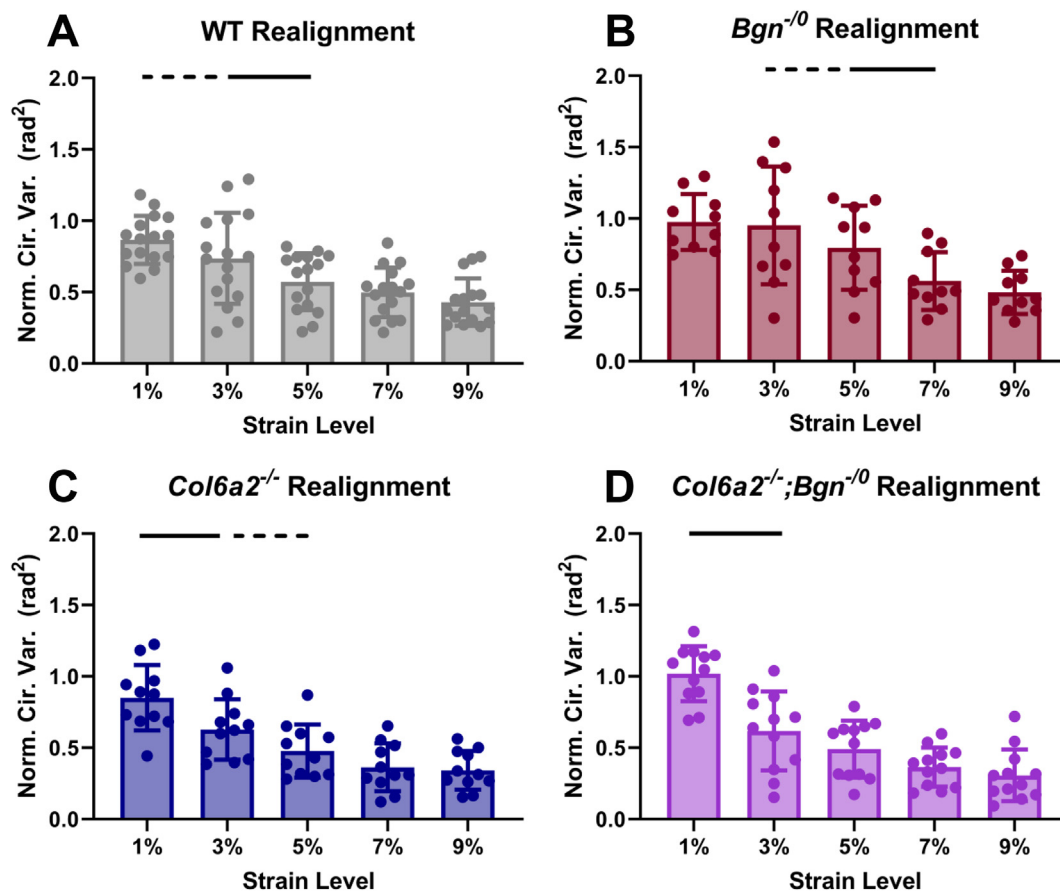
Fig. 7. Fiber realignment during ramp to failure. (A) WT tendons realigned between 3% and 5% strain. (B) *Col6a2*^{-/-} tendons realigned earlier than WT tendons, between 1% and 3% strain. (C) *Bgn*[-/0] tendons realigned later than WT tendons, between 5% and 7% strain. (D) *Col6a2*^{-/-};*Bgn*[-/0] tendons realigned earlier than WT tendons, between 1% and 3% strain. Solid bars indicate $p < 0.05$, and dashed bars indicate $p < 0.1$ from one-way repeated measures ANOVAs with Tukey post-hoc comparisons.

work resembles the *in situ* structure of the tendon PCM, of which collagen VI is a large component [31]. This study demonstrated co-expression and co-localization of these molecules in healing tendon, providing further evidence of their interaction. Assuming this model of the tendon PCM, the PCM may be analogous to a "house of cards" that is taped together. In this analogy, biglycan serves as the stabilizing "tape" and without "tape", the struc-

ture is unstable and more easily perturbed. While this has a deleterious effect on tendon function, absence of the "house of cards" altogether would have a larger effect than absence of the binding "tape" alone. This may be why the collagen VI knockout led to more severe functional deficits – the PCM was disrupted beyond the "destabilization" seen with biglycan knockout. This model would also explain the similar tendon out-

comes observed between the collagen VI single knockout and the collagen VI/biglycan double knockout. Since the main structure of the PCM is already absent in the collagen VI knockout, the additional knockout of biglycan does not result in further robust changes, as biglycan's role in organizing the PCM is less relevant. This paradigm of co-dependent function likely holds true during tendon regeneration, where we found co-expression and co-induction of collagen VI and biglcyan through the tendon healing process.

While the focus of this report was on the role of collagen VI α2 and biglycan on the structure and function of tendons, it is important to consider what role different chains of collagen VI (i.e., *Col6a5* and *Col6a6*) or other SLRPs have in tendon biology. In addition to this, the possible interface with other molecular influences such as TGF-β must also be considered. Sabetelli et al, showed that TGF-β1 differentially regulates collagen VI α5 and α6 chains in human tendon cultures [41]. Biglycan is also affected by TGF-β activity in healing tendons [42]. In this context, it is interesting to speculate that a TGF-β loop controls many aspects of tendon healing related to matrix biology, including the production of collagen VI chains, biglycan, and potentially other SLRPs. Future studies are needed to determine if or how different collagen VI chains are affected during tendon healing and how this in turn could affect tendon structure and function. (NEW PARAGRAPH) By examining mRNA expressed during tendon healing, we found that mRNA encoding *Bgn* is expressed at a 10x higher FPKM level than mRNA encoding *Col6a1*, *Col6a2* or *Col6a3*. It is not known at this time if the mRNA in question is translated into protein. However, it is likely that the relative molecular presence of biglycan is much higher than that of collagen VI in healing tendons. To determine if this phenomena is specific to tendon, we examined relative mRNA ratios in age and gender matched WT bones and found *Bgn* mRNA is also 10x more abundant than that of *Col6a1*, *Col6a2*, or *Col6a3* [43]. The ramification of this observation is not clear and will require further investigation to fully understand its functional consequences. (NEW PARAGRAPH) An important cellular aspect not addressed in the manuscript is the possible role of biglycan and collagen VI in modulating macrophage function during tendon healing. Previous work shows biglycan can control macrophage function via CD14 activation [44]. In kidney disease, biglycan appears to regulate macrophage autophagy through molecular interactions involving the CD44/Toll-like Receptor4 axis [45]. Interestingly, other work shows there is an increased number of M1 macrophages in the first two weeks after tendon injury and a subsequent increase of M2 macrophages during regeneration [46], suggesting that subsets of macrophages may have different functions during tendon healing. Considering collagen

VI is abundantly produced by M2 polarized macrophages [47], it is tempting to speculate that collagen VI plays roles in tendon repair related to M2 function. It will be interesting to determine the expression pattern of biglycan and collagen VI during macrophage infiltration in the tendon injury model and, further, to see if the absence of the biglycan, collagen VI, or both could influence macrophage function during tendon healing.

In conclusion, our data clearly demonstrates distinct and non-additive roles for biglycan and collagen VI in regulating tendon function. Understanding more about their functions in tendon homeostasis could provide a foundation for therapeutics that aim to restore tendon function following injury or degeneration.

Experimental procedures

Mice

All animal treatment and care conformed to NIH guidelines and were approved by Carnegie Institution Animal Care and Use Committee (ACUC) for the tendon repair model and the NIH-DIR ACUC (#18–865) for TEM and biomechanical studies. C57BL6/J strain (WT) was purchased from Jackson Laboratory. Male WT mice were used for deep RNA-seq and injuries for immunohistochemical presentation. Wild-type, *Col6a2*$^{-/-}$, *Bgn*$^{-/0}$ and *Col6a2*$^{-/-}$;*Bgn*$^{-/0}$ mice derived either in house (*Bgn*$^{-/0}$, [37]) or in the lab of Carsten Bonnemann (NINDS, NIH-DIR) (*Col6a2*$^{-/-}$).

Deep RNA-seq

For injured/regenerated samples, whole patellar tendon pairs were isolated in triplicate. Samples were collected during the same time window to mitigate any batch effects. Isolated tendons pairs were minced with dissecting scissors, transferred to 15 mL conical tubes containing prewarmed 10 mL of 1X PBS (Gibco), 4 mg/mL dispase II (Sigma), and 3 mg/mL collagenase (Worthington). Conical tubes were transferred and positioned horizontally in a shaking 37 °C water bath for 1.5hr. Following this, enzymes were deactivated with 3 mL TSPC specialized media, run through a 40 μm filter, and pelleted at 300xg for 30′ @ 4 °C. The cell pellet was washed with 1 mL 1X PBS (Gibco) and re-pelleted at 300xg for 15′ @ 4 °C. The cell pellet was subsequently lysed for RNA preparation using the RNA Direct-zol kit (Zymo), followed by Ovation RNA-seq V2 System (NuGEN) to generate cDNAs. cDNAs were then sonicated to 300–500 bp range (Covaris) and libraries were generated by the TruSeq RNA Library Prep Kit (Illumina) for single-end 75 bp reads (Next-seq, Illumina). Reads were mapped and aligned to the mm10 reference genome using TopHat [48]. Read count normalization was determined by HTSeq [49] and differential expression

analysis across the temporal samples was assessed by the R package, DESeq [50]. Normalized, relative count data are represented as FPKM values in visualizations using GraphPad.

RNA-seq data

The raw RNA-seq data will be submitted to NCBI GEO and released upon acceptance for publication.

NCBI BioSample: will be released upon manuscript acceptance.

Patellar biopsy punch surgical procedure

Bilateral biopsy punch was performed as described previously [36] with the following modifications: A #5 forcep (Dupont) was used to expose the underside of the patellar tendon. A small, thin metal sheet was placed underneath the tendon to provide a backing for the excisional biopsy punch. An Accu-Sharp Punch MII 0.75 mm diameter (Shoney Scientific) was used. Skin lesion was closed using sutures (Ethicon, PERMA-HANDTMSilk, 5–0, P-3). Mice were placed in a heated chamber to recover from anesthesia. Elizabethan collars were put on the mice for the first 3 days following operation. Knee joints were harvested for assay at specified time points for assays. Knee joints were harvested for analysis at specified time points for the assays performed. For immunohistochemistry, samples were collected 3 days post-surgury prior to processing.

Tissue preparation and cryo-sectioning

Knee joints were dissected out in PBS (Gibco) as described [51] with modifications described [36]: Twenty μm sagittal sections were collected on Cryofilm Type IIC (Section Lab, Inc., Japan) and affixed to glass slides using 1.5% chitosan in 0.25% acetic acid and allowed to dry at 4 °C before use. Sections throughout the tendon were collected.

Immunohistochemistry

Dried sections were hydrated with PBS, permeabilized 15′ with PBS plus 0.5% Triton X-100 (w/v; 0.5% PBT), rinsed with 0.05% PBT, and then treated with ABCase (per manufacturer guidelines) for 1 h @ 37 °C. Following this, they were rinsed with PBT 2X for 5′, endogenous peroxidase activity was quenched with 3% H_2O_2 in PBS for 10′, and next rinsed with PBT 2X for 5′. Slides were subsequently treated for 1 h @ 37 °C with 10% normal goat serum in PBS. Serial sections were incubated with primary antibodies diluted in ABC blocking solution (Vector Labs) overnight at 4 °C. Primary antibodies used were rabbit anti-Collagen VI: 1:200 dilution (70R-CR009x, Fitzgerald, USA) rabbit anti- Bgn (in house made: LF-159): 1:500 dilution. Negative controls were 1:200 dilution of rabbit IgG 1:500 dilution of normal rabbit serum respectively.

Following primary incubation, slides were washed with 0.05% PBT 3-5X for 5′ each, Avidin/Biotin Block (Vector Labs, according to manufacturer), followed by a quick rinse with PBT. Sections were then incubated for 30′ with diluted biotinylated, goat anti-rabbit secondary antibody (Vectastain by Vector), washed 3X with PBT, and subsequently incubated for 30′ with Vectastain ABC reagent (Vector). Following formation of the super complex, slides were washed 3X with PBT, then incubated with DAB substrate (Vector) for immunohistochemistry until color developed. Lastly, slides were washed with PBT 5X for 5′ each to quench reaction. Sections were counterstained with Gill's Hematoxylin (Vector) for 15′ according to manufacturer. Sections were dehydrated through a graded ethanol series (50, 75, 95, 100, 100 %, then Xylene; 30″ each) and mounted with Permamount (EMS)

Images were taken on a Nikon Eclipse E800 scope equipped with Plan Fluor Apo objectives (magnification/numerical aperture; 4x/0.13, 10x/0.45, 20x/0.75) and captured with a Canon EOS Rebel T3i camera and EOS Utility software.

Transmission electron microscopy

Flexor digitorum longus (FDL) tendons from 60 day-old mice (n = 4 tendons/genotype from minimum of n = 3 mice/genotype) were prepared for analysis of fibril structure by transmission electron microscopy as previously described [52,53]. Tendon samples were collected in the morning hours (8AM-12PM local time) to mitigate any effects of circadian regulation on collagen fibril size [54]. Briefly, tendons were fixed in 4% paraformaldehyde, 2.5% glutaraldehyde, 0.1 M sodium cacodylate and 8 mM CaCl2, adjusted to pH 7.4 with NaOH, then post-fixed with 1% osmium tetroxide, dehydrated with an ethanol series, embedded in Epon 812 and polymerized at 60 °C. Ultra-thin cross-sections of were imaged on a JEOL 1400 transmission electron microscope (JEOL Ltd., Tokyo, Japan) equipped with a Gatan Orius wide-field side mount CC Digital camera (Gatan Inc., Pleasanton, CA). Digital images (n = 32/tendon) from the mid-substance of each tendon were taken from non-overlapping areas at 60,000X. Images were randomized and masked before fibril diameters were measured using an RM Biometrics-Bioquant Image Analysis System (Nashville, TN). A region of interest (ROI) of appropriate size was determined within each digital image. All fibrils in the region of interest were measured and 33–63 regions of interest were used to collect at least 80 fibril diameter measurements per image. Fibril diameters (2691–3288 depending on genotype) were measured along the minor axis of the fibril cross-section. Fibril diameter measurements from tendon of each genotype were pooled and graphed by histogram in 5 nm bins (x-axis) vs frequency (%, y-axis) and displayed by box-plot. A two-sample

Kolmogorov–Smirnov (K-S) test ($p < 0.05$) was used to assess sameness of the distributions between genotypes. Mean fibril density was presented by tendon in a dot-chart and paired Student's *t*-test ($p < 0.05$) was used to assess for significance between genotypes.

Biomechanical testing

To assess FDL tendon mechanical properties, two month-old male wild-type (WT) (n = 16), $Col6a2^{-/-}$ (n = 11), $Bgn^{-/0}$ (n = 12), and $Col6a2^{-/-}$; $Bgn^{-/0}$ (n = 13) mice were used. FDL tendons were dissected from the left hind limb and the tendon sheath fine dissected off the tendon. Tendon cross-sectional area (CSA) was measured with a custom laser device, and stain lines were applied for optical tracking [55]. The FDL tendon was gripped with sandpaper, leaving a 5 mm gauge length. This gauge length spans the main body of the tendon, starting at the convergence of the tendon digits and ending near the myotendinous junction.

For biomechanical testing, samples were loaded in a phosphate buffered saline bath within a uniaxial tensile testing machine (Instron 5542, Instron, Norwood, MA). The testing protocol consisted of 10 cycles of preconditioning between 0.01 and 0.02 N at 1 Hz, a 5-minute hold, a 5% stress relaxation for 10 min, a 1-minute hold, and a ramp to failure at 0.5% strain/s. Stress relaxation, stiffness, and maximum load were computed from force-displacement data. Modulus and maximum stress were computed using optical tracking and normalization to CSA. Dynamic collagen fiber realignment was measured throughout the ramp-to-failure test using a crossed polarizer setup [56].

For mechanical properties, a one-way ANOVA with Bonferroni post-hoc tests was used to compare across genotypes. For fiber realignment data, a two-way ANOVA with Tukey correction for multiple comparisons was used to compare across genotype and strain. Significance was set at $p < 0.05$, and trends were set at $p < 0.1$.

CRediT authorship contribution statement

Ryan J. Leiphart: Conceptualization, Methodology, Investigation, Formal analysis, Writing – original draft, Writing – review & editing. **Hai Pham:** Conceptualization, Investigation. **Tyler Harvey:** Conceptualization, Methodology, Investigation, Formal analysis, Writing – review & editing, Writing – original draft. **Taishi Komori:** Methodology, Investigation. **Tina M. Kilts:** Investigation. **Snehal S. Shetye:** Methodology. **Stephanie N. Weiss:** Investigation. **Sheila M. Adams:** Methodology, Investigation, Formal analysis. **David E. Birk:** Conceptualization, Methodology, Formal analysis, Writing – original draft, Writing – review & editing. **Louis J. Soslowsky:** Conceptualization. **Marian F. Young:** Conceptualization, Supervision, Writing – original draft.

DECLARATION OF COMPETING INTEREST

The authors declare that they have no known competing financial interests or personal relationships that could have appeared to influence the work reported in this paper.

[1] Co-first authors.

References

[1]. Magnan, B., Bondi, M., Pierantoni, S., Samaila, E., (2014). The pathogenesis of Achilles tendinopathy: A systematic review. *Foot Ankle Surg.*, **20** (3), 154–159. https://doi.org/10.1016/j.fas.2014.02.010.

[2]. Lewis, J.S., (2009). Rotator cuff tendinopathy. *Br. J. Sports Med.*, **43** (4), 236–241. https://doi.org/10.1136/bjsm.2008.052175.

[3]. Magra, M., Maffulli, N., (2008). Genetic aspects of tendinopathy. *J. Sci. Med. Sport.*, **11** (3), 243–247. https://doi.org/10.1016/j.jsams.2007.04.007.

[4]. H.R.C. Screen, D.E. Berk, K.E. Kadler, F. Ramirez, M.F. Young, Tendon functional extracellular matrix, in: J. Orthop. Res., John Wiley and Sons Inc., 2015: pp. 793–799. https://doi.org/10.1002/jor.22818.

[5]. D.F. Holmes, Y. Lu, T. Starborg, K.E. Kadler, Collagen Fibril Assembly and Function, in: Curr. Top. Dev. Biol., Academic Press Inc., 2018: pp. 107–142. https://doi.org/10.1016/bs.ctdb.2018.02.004

[6]. Mienaltowski, M.J., Birk, D.E., (2014). Structure, Physiology, and Biochemistry of Collagens. *Adv. Exp. Med. Biol., Adv Exp Med Biol,*, 5–29. https://doi.org/10.1007/978-94-007-7893-1_2.

[7]. Robinson, K.A., Sun, M., Barnum, C.E., Weiss, S.N., Huegel, J., Shetye, S.S., Lin, L., Saez, D., Adams, S.M., Iozzo, R.V., Soslowsky, L.J., Birk, D.E., (2017). Decorin and biglycan are necessary for maintaining collagen fibril structure, fiber realignment, and mechanical properties of mature tendons. *Matrix Biol.*, **64**, 81–93. https://doi.org/10.1016/j.matbio.2017.08.004.

[8]. Ameye, L., Aria, D., Jepsen, K., Oldberg, A., Xu, T., Young, M.F., (2002). Abnormal collagen fibrils in tendons of biglycan/fibromodulin-deficient mice lead to gait impairment, ectopic ossification, and osteoarthritis. *FASEB J.*, **16** (7), 673–680. https://doi.org/10.1096/fj.01-0848com.

[9]. Ansorge, H.L., Meng, X., Zhang, G., Veit, G., Sun, M., Klement, J.F., Beason, D.P., Soslowsky, L.J., Koch, M., Birk, D.E., (2009). Type XIV collagen regulates fibrillogenesis: Premature collagen fibril growth and tissue dysfunction in null mice. *J. Biol. Chem.*, **284** (13), 8427–8438. https://doi.org/10.1074/jbc.M805582200.

[10]. Eekhoff, J.D., Steenbock, H., Berke, I.M., Brinckmann, J., Yanagisawa, H., Wagenseil, J.E., Lake, S.P., (2021). Dysregulated assembly of elastic fibers in fibulin-5 knockout mice results in a tendon-specific increase in elastic modulus. *J. Mech. Behav. Biomed. Mater.*, **113**, 104134. https://doi.org/10.1016/j.jmbbm.2020.104134.

[11]. Chen, S., Birk, D.E., (2013). The regulatory roles of small leucine-rich proteoglycans in extracellular matrix assembly. *FEBS J.*, **280** (10), 2120–2137. https://doi.org/10.1111/febs.12136.

[12]. Schaefer, L., Iozzo, R.V., (2008). Biological functions of the small leucine-rich proteoglycans: From genetics to signal transduction. *J. Biol. Chem.*, **283** (31), 21305–21309. https://doi.org/10.1074/jbc.R800020200.

[13]. Nastase, M.V., Young, M.F., Schaefer, L., (2012). Biglycan: A Multivalent Proteoglycan Providing Structure and Signals. *J. Histochem. Cytochem.*, **60** (12), 963–975. https://doi.org/10.1369/0022155412456380.

[14]. Corsi, A., Xu, T., Chen, X.-D., Boyde, A., Liang, J., Mankani, M., Sommer, B., Iozzo, R.V., Eichstetter, I., Robey, P.G., Bianco, P., Young, M.F., (2002). Phenotypic Effects of Biglycan Deficiency Are Linked to Collagen Fibril Abnormalities, Are Synergized by Decorin Deficiency, and Mimic Ehlers-Danlos-Like Changes in Bone and Other Connective Tissues. *J. Bone Miner. Res.*, **17** (7), 1180–1189. https://doi.org/10.1359/jbmr.2002.17.7.1180.

[15]. Gordon, J.A., Freedman, B.R., Zuskov, A., Iozzo, R.V., Birk, D.E., Soslowsky, L.J., (2015). Achilles tendons from decorin- and biglycan-null mouse models have inferior mechanical and structural properties predicted by an image-based empirical damage model. *J. Biomech.*, **48** (10), 2110–2115. https://doi.org/10.1016/j.jbiomech.2015.02.058.

[16]. Buckley, M.R., Huffman, G.R., Iozzo, R.V., Birk, D.E., Soslowsky, L.J., (2013). The location-specific role of proteoglycans in the flexor carpi ulnaris tendon. *Connect. Tissue Res.*, **54** (6), 367–373. https://doi.org/10.3109/03008207.2013.832232.

[17]. Dourte, L.M., Pathmanathan, L., Mienaltowski, M.J., Jawad, A.F., Birk, D.E., Soslowsky, L.J., (2013). Mechanical, compositional, and structural properties of the mouse patellar tendon with changes in biglycan gene expression. *J. Orthop. Res.*, **31** (9), 1430–1437. https://doi.org/10.1002/jor.22372.

[18]. Kilts, T., Ameye, L., Syed-Picard, F., Ono, M., Berendsen, A.D., Oldberg, A., Heegaard, A.M., Bi, Y., Young, M.F., (2009). Potential roles for the small leucine-rich proteoglycans biglycan and fibromodulin in ectopic ossification of tendon induced by exercise and in modulating rotarod performance. *Scand. J. Med. Sci. Sport.*, **19**, 536–546. https://doi.org/10.1111/j.1600-0838.2009.00909.x.

[19]. Robinson, P.S., Huang, T.F., Kazam, E., Iozzo, R.V., Birk, D.E., Soslowsky, L.J., (2005). Influence of decorin and biglycan on mechanical properties of multiple tendons in knockout mice. *J. Biomech. Eng.*, **127**, 181–185. https://doi.org/10.1115/1.1835363.

[20]. Bi, Y., Ehirchiou, D., Kilts, T.M., Inkson, C.A., Embree, M.C., Sonoyama, W., Li, L.i., Leet, A.I., Seo, B.-M., Zhang, L.i., Shi, S., Young, M.F., (2007). Identification of tendon stem/progenitor cells and the role of the extracellular matrix in their niche. *Nat. Med.*, **13** (10), 1219–1227. https://doi.org/10.1038/nm1630.

[21]. Cescon, M., Gattazzo, F., Chen, P., Bonaldo, P., (2015). Collagen VI at a glance. *J. Cell Sci.*, **128**, 3525–3531. https://doi.org/10.1242/jcs.169748.

[22]. Bonaldo, P., Russo, V., Bucciotti, F., Doliana, R., Colombatti, A., (1990). Structural and Functional Features of the α3 Chain Indicate a Bridging Role for Chicken Collagen VI in Connective Tissues. *Biochemistry.*, **29**, 1245–1254. https://doi.org/10.1021/bi00457a021.

[23]. Bidanset, D.J., Guidry, C., Rosenberg, L.C., Choi, H.U., Timpl, R., Hook, M., (1992). Binding of the proteoglycan decorin to collagen type VI. *J Biol Chem.*, **267** (8), 5250–5256.

[24]. Wiberg, C., Hedbom, E., Khairullina, A., Lamandé, S.R., Oldberg, Å., Timpl, R., Mörgelin, M., Heinegård, D., (2001). Biglycan and decorin bind close to the n-terminal region of the collagen VI triple helix. *J. Biol. Chem.*, **276** (22), 18947–18952. https://doi.org/10.1074/jbc.M100625200.

[25]. Izu, Y., Ansorge, H.L., Zhang, G., Soslowsky, L.J., Bonaldo, P., Chu, M.-L., Birk, D.E., (2011). Dysfunctional tendon collagen fibrillogenesis in collagen VI null mice. *Matrix Biol.*, **30** (1), 53–61. https://doi.org/10.1016/j.matbio.2010.10.001.

[26]. Wilusz, R.E., Sanchez-Adams, J., Guilak, F., (2014). The structure and function of the pericellular matrix of articular cartilage. *Matrix Biol.*, **39**, 25–32. https://doi.org/10.1016/j.matbio.2014.08.009.

[27]. Thakkar, D., Grant, T.M., Hakimi, O., Carr, A.J., (2014). Distribution and expression of type VI collagen and elastic fibers in human rotator cuff tendon tears. *Connect. Tissue Res.*, **55** (5-6), 397–402. https://doi.org/10.3109/03008207.2014.959119.

[28]. Carvalho, H.F., Felisbino, S.L., Keene, D.R., Vogel, K.G., (2006). Identification, content, and distribution of type VI collagen in bovine tendons. *Cell Tissue Res.*, **325** (2), 315–324. https://doi.org/10.1007/s00441-006-0161-0.

[29]. Bushby, K.M.D., Collins, J., Hicks, D., (2014). Collagen Type VI Myopathies. *Adv. Exp. Med. Biol.,,,*, 185–199. https://doi.org/10.1007/978-94-007-7893-1_12.

[30]. Wiberg, C., Heinegård, D., Wenglén, C., Timpl, R., Mörgelin, M., (2002). Biglycan Organizes Collagen VI into Hexagonal-like Networks Resembling Tissue Structures. *J. Biol. Chem.*, **277** (51), 49120–49126. https://doi.org/10.1074/jbc.M206891200.

[31]. Ritty, T.M., Roth, R., Heuser, J.E., (2003). Tendon cell array isolation reveals a previously unknown fibrillin-2-containing macromolecular assembly. *Structure.*, **11** (9), 1179–1188. https://doi.org/10.1016/S0969-2126(03)00181-3.

[32]. Huang, A.H., Lu, H.H., Schweitzer, R., (2015). Molecular regulation of tendon cell fate during development in: J. Orthop. Res.. John Wiley and Sons Inc., pp. 800–812. https://doi.org/10.1002/jor.22834.

[33]. Dyment, N.A., Galloway, J.L., (2015). Regenerative biology of tendon: mechanisms for renewal and repair. *Curr. Mol. Biol. Reports.*, **1** (3), 124–131. https://doi.org/10.1007/s40610-015-0021-3.

[34]. Harvey, T., Fan, C.-M., (2018). Origin of tendon stem cells in situ. *Front. Biol. (Beijing)*, **13** (4), 263–276. https://doi.org/10.1007/s11515-018-1504-4.

[35]. Beason, D.P., Kuntz, A.F., Hsu, J.E., Miller, K.S., Soslowsky, L.J., (2012). Development and evaluation of multiple tendon injury models in the mouse. *J. Biomech.*, **45** (8), 1550–1553. https://doi.org/10.1016/j.jbiomech.2012.02.022.

[36]. Harvey, T., Flamenco, S., Fan, C.-M., (2019). A Tppp3 + Pdgfra + tendon stem cell population contributes to regeneration and reveals a shared role for PDGF signalling in regeneration and fibrosis. *Nat. Cell Biol.*, **21** (12), 1490–1503. https://doi.org/10.1038/s41556-019-0417-z.

[37]. Xu, T., Bianco, P., Fisher, L.W., Longenecker, G., Smith, E., Goldstein, S., Bonadio, J., Boskey, A., Heegaard, A.-M., Sommer, B., Satomura, K., Dominguez, P., Zhao, C., Kulkarni, A.B., Robey, P.G., Young, M.F., (1998). Targeted disruption of the biglycan gene leads to an osteoporosis-like phenotype in mice. *Nat. Genet.*, **20** (1), 78–82. https://doi.org/10.1038/1746.

[38]. Pham, H.T., Kram, V., Dar, Q.A., Komori, T., Ji, Y., Mohassel, P., Rooney, J., Li, L., Kilts, T.M., Bonnemann, C., Lamande, S., Young, M.F., (2020). Collagen VIα2 chain deficiency causes trabecular bone loss by potentially promoting osteoclast differentiation through enhanced TNFα signaling. *Sci. Rep.*, **10**, 1–14. https://doi.org/10.1038/s41598-020-70730-7.

[39]. Liu, H., Xu, J., Liu, C.-F., Lan, Y., Wylie, C., Jiang, R., (2015). Whole transcriptome expression profiling of mouse limb tendon development by using RNA-seq. *J. Orthop. Res.*, **33**, 840. https://doi.org/10.1002/JOR.22886.

[40]. Zhang, G., Ezura, Y., Chervoneva, I., Robinson, P.S., Beason, D.P., Carine, E.T., Soslowsky, L.J., Iozzo, R.V., Birk, D.E., (2006). Decorin regulates assembly of collagen fibrils and acquisition of biomechanical properties during tendon development. *J. Cell. Biochem.*, **98** (6), 1436–1449.

[41]. Sabatelli, P., Sardone, F., Traina, F., Merlini, L., Santi, S., Wagener, R., Faldini, C., (2016). TGF-β1 differentially modulates the collagen VI α5 and α6 chains in human tendon cultures accessed December 7, 2021 *J. Biol. Regul. Homeost. Agents.*, **30**, 107–113 https://pubmed.ncbi.nlm.nih.gov/28002907/.

[42]. Farhat, Y.M., Al-Maliki, A.A., Chen, T., Juneja, S.C., Schwarz, E.M., O'Keefe, R.J., Awad, H.A., Agarwal, S., (2012). Gene Expression Analysis of the Pleiotropic Effects of TGF-β1 in an In Vitro Model of Flexor Tendon Healing. *PLoS One.*, **7** (12), e51411.

[43]. Pham, H.T., Kram, V., Dar, Q.A., Komori, T., Ji, Y., Mohassel, P., Rooney, J., Li, L., Kilts, T.M., Bonnemann, C., Lamande, S., Young, M.F., (2020). Collagen VIα2 chain deficiency causes trabecular bone loss by potentially promoting osteoclast differentiation through enhanced TNFα signaling. *Sci. Reports*, **101** (10), 2020–pp. 1–14. https://doi.org/10.1038/s41598-020-70730-7.

[44]. Roedig, H., Nastase, M.V., Frey, H., Moreth, K., Zeng-Brouwers, J., Poluzzi, C., Hsieh, L.T.H., Brandts, C., Fulda, S., Wygrecka, M., Schaefer, L., (2019). Biglycan is a new high-affinity ligand for CD14 in macrophages. *Matrix Biol.*, **77**, 4–22. https://doi.org/10.1016/J.MATBIO.2018.05.006.

[45]. Poluzzi, C., Nastase, M.V., Zeng-Brouwers, J., Roedig, H., Hsieh, L.T.H., Michaelis, J.B., Buhl, E.M., Rezende, F., Manavski, Y., Bleich, A., Boor, P., Brandes, R.P., Pfeilschifter, J., Stelzer, E.H.K., Münch, C., Dikic, I., Brandts, C., Iozzo, R.V., Wygrecka, M., Schaefer, L., (2019). Biglycan evokes autophagy in macrophages via a novel CD44/Toll-like receptor 4 signaling axis in ischemia/reperfusion injury. *Kidney Int.*, **95**, 540–562. https://doi.org/10.1016/J.KINT.2018.10.037.

[46]. Sunwoo, J.Y., Eliasberg, C.D., Carballo, C.B., Rodeo, S.A., (2020). The role of the macrophage in tendinopathy and tendon healing. *J. Orthop. Res.*, **38** (8), 1666–1675.

[47]. Chen, P., Cescon, M., Zuccolotto, G., Nobbio, L., Colombelli, C., Filaferro, M., Vitale, G., Feltri, M.L., Bonaldo, P., (2015). Collagen VI regulates peripheral nerve regeneration by modulating macrophage recruitment and polarization. *Acta Neuropathol.*, **129** (1), 97–113.

[48]. Trapnell, C., Roberts, A., Goff, L., Pertea, G., Kim, D., Kelley, D.R., Pimentel, H., Salzberg, S.L., Rinn, J.L., Pachter, L., (2012). Differential gene and transcript expression analysis of RNA-seq experiments with TopHat and Cufflinks. *Nat. Protoc.*, **7** (3), 562–578.

[49]. Anders, S., Pyl, P.T., Huber, W., (2015). HTSeq—a Python framework to work with high-throughput sequencing data. *Bioinformatics.*, **31** (2), 166–169.

[50]. Anders, S., Huber, W., (2010). Differential expression analysis for sequence count data. *Genome Biol.*, **1110** (11) https://doi.org/10.1186/GB-2010-11-10-R106.

[51]. Dyment, N.A., Liu, C.-F., Kazemi, N., Aschbacher-Smith, L.E., Kenter, K., Breidenbach, A.P., Shearn, J.T., Wylie, C., Rowe, D.W., Butler, D.L., Mezey, E., (2013). The Paratenon Contributes to Scleraxis-Expressing Cells during Patellar Tendon Healing. *PLoS One.*, **8** (3), e59944. https://doi.org/10.1371/journal.pone.0059944.

[52]. Birk, D.E., Trelstad, R.L., (1984). Extracellular compartments in matrix morphogenesis: Collagen fibril, bundle, and lamellar formation by corneal fibroblasts. *J. Cell Biol.*, **99**, 2024–2033. https://doi.org/10.1083/jcb.99.6.2024.

[53]. Dunkman, A.A., Buckley, M.R., Mienaltowski, M.J., Adams, S.M., Thomas, S.J., Satchell, L., Kumar, A., Pathmanathan, L., Beason, D.P., Iozzo, R.V., Birk, D.E., Soslowsky, L.J., (2013). Decorin expression is important for age-related changes in tendon structure and mechanical properties. *Matrix Biol.*, **32** (1), 3–13. https://doi.org/10.1016/j.matbio.2012.11.005.

[54]. Chang, J., Garva, R., Pickard, A., Yeung, C.-Y., Mallikarjun, V., Swift, J., Holmes, D.F., Calverley, B., Lu,

Y., Adamson, A., Raymond-Hayling, H., Jensen, O., Shearer, T., Meng, Q.J., Kadler, K.E., (2020). Circadian control of the secretory pathway maintains collagen homeostasis. *Nat. Cell Biol.*, **22** (1), 74–86. https://doi.org/10.1038/s41556-019-0441-z.

[55]. Favata, M., (2006). Scarless healing in the fetus: Implications and strategies for postnatal tendon repair. Diss, Available from ProQuest. https://repository.upenn.edu/dissertations/AAI3246156 (accessed February 19, 2020.

[56]. Lake, S.P., Miller, K.S., Elliott, D.M., Soslowsky, L.J., (2009). Effect of fiber distribution and realignment on the nonlinear and inhomogeneous mechanical properties of human supraspinatus tendon under longitudinal tensile loading. *J. Orthop. Res.*, **27** (12), 1596–1602. https://doi.org/10.1002/jor.20938.